

# Transient Underwater Acoustic Channel Simulator Development

Michael S Caley (1) and Alec J Duncan (1)

(1) Curtin University, Department of Imaging and Applied Physics, Centre for Marine Science and Technology, Perth, Australia

## ABSTRACT

The underwater communication channel is often characterised by transient reinforcement and fading of multiple transmission paths, such that no single transmission path can be generally relied upon to provide a continuous communication channel. For smooth to moderate seas the transient real ocean channel may be conceptualised as a time-series of static channel ‘snap-shots’. For a static channel geometry and transmission medium, ray-tracing methods enable calculation of the channel impulse response for the relatively high frequencies associated with data communications. This leads to the modelling challenge of how a series of static channel responses may be seamlessly joined to create a transient channel response simulation that achieves realistic multi-path fading, and arrival time spreading (or synonymously Doppler frequency spreading) of an arbitrary communications signal. This paper describes algorithms that have been explored to identify emergent, continuing and extinguishing channel transmission paths from one ‘snapshot’ impulse response to the next. The calculation architecture being developed to simulate the transient channel response is described.

## INTRODUCTION

In 2011 the Department of Electrical and Computer Engineering and the Centre for Marine Science and Technology (CMST) at Curtin University commenced a project to develop high-rate underwater acoustic communications simulator to support developing ocean-based industries in Australia (Nordholm et al., 2010). The purpose of the simulator is to simulate the way that the real ocean produces transient distortion of acoustic communication signals between a transmitter and a receiver. The simulator is intended to provide a configurable analogue of the real ocean that can be used to improve understanding of the influence of the marine acoustic environment on communications signals, and assist the development of underwater communication modulation and demodulation algorithms and hardware.

Transient phenomena that are key to the development of a high fidelity acoustic channel simulator are the transient delay and Doppler frequency spreading of the received signal imparted by the moving sea-surface, shown schematically in Fig. 1, and the transient Doppler imparted by moving transmitter and/or receiver platforms (Eggen et al., 2000, van Walree et al., 2008).

### Conceptual multi-path transmission

In Fig. 1, the acoustic transmission paths that are surface or bottom-reflected travel greater distance than the direct path, resulting in a delayed pulse arrival relative to the pulse that travels via the direct path. Additionally, as the acoustic reflection point on the undulating sea-surface moves, the surface-reflected transmission paths modulate in path length, resulting in fluctuations in the delay (or time-of-flight) of successive pulses relative to the direct path. Also, the ‘stretching’ or ‘compression’ of the delay results in Doppler frequency shifts of the transmitted acoustic wave. In the figure ‘stretching’ is shown by the red acoustic wave-fronts, and ‘compression’ by the blue wave-front.

The diagram in Fig. 1 is over-simplified, to illustrate the concept of delayed paths relative to a direct path. In doing so the diagram implies an iso-velocity sound-speed environment as

there is no curvature of the sound ray-paths. In real marine channels it is not uncommon for upward or downward refracting sound-speed gradients to exist that curve transmission paths, which may preclude any direct path transmission. In this situation the signal transmitted via reflected paths is essential for communication. Another important aspect of the multi-path physics that is not conveyed by Fig. 1 is the common occurrence of destructive phase interference between paths which may have similar amplitude and close to 180° relative phase. This may also substantially degrade the direct path signal propagation.

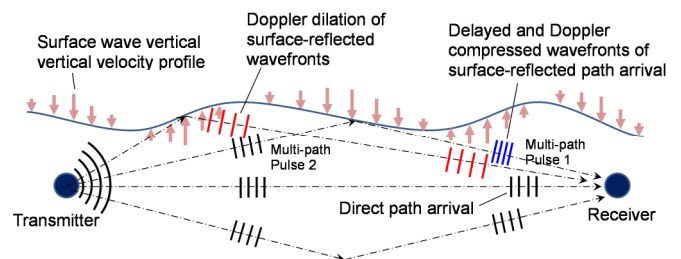


Figure 1. Conceptual signal Doppler shift and path delay

### Path fading and delay spreading in a real ocean channel

An experimental channel acoustic response history obtained over 500 m range in 13.5 m water depth is presented in Fig. 2 to provide an example of the often discontinuous nature of the underwater channel on any particular transmission path. Analysis of the channel Doppler and delay spreading for this experimental work is described in (Caley and Duncan, 2013). The plot in Fig. 2 represents 1400 successive channel responses determined by repeatedly transmitting a 21 ms length probe signal followed by cross-correlation of the probe signal with the measured received signal.

The first correlation maxima (vertical band occurring at 0 ms on the delay x-axis) represents the combination of the direct and bottom-reflected paths. Continuity of this band in the y-axis direction indicates a persistent or stable signal arrival via the direct path. From analysis it was determined that this first signal arrival was suppressed in strength (relative to the next

band at later delay comprised of single surface reflected paths) by destructive interference between the direct and bottom-reflected transmission path. At some points in the time history it may be noted that the first arrival effectively vanishes.

The bands of correlation strength at greater delays (x-axis) are increasingly discontinuous in the time dimension (y-axis), due to decreasing stability of signal transmission paths involving additional surface reflections.

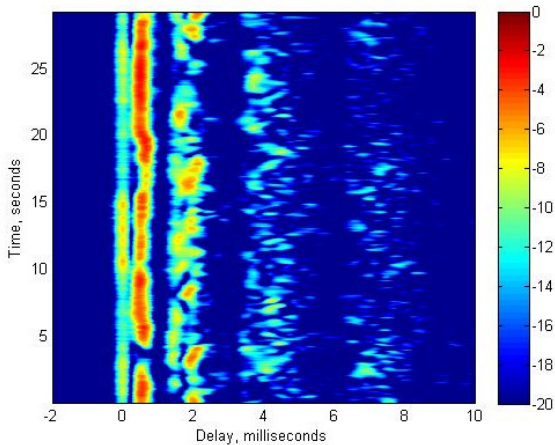


**Figure 2.** Experimental transmit-receive channel response history(dB) from successive 21 ms pulse sequences– recorded over 500 m range

The phenomenon of path delay spreading can be illustrated by contrasting the real dynamic channel response in Fig. 2 to the static channel response history illustrated in Fig. 3 that would result for the same 500 m range but with a stationary transmitter (no drift) and a flat sea surface. At each instant in time (y-axis) in Fig. 3 the delay structure (x-axis) of direct and reflected path arrivals is fixed. The static channel by definition exhibits no delay spreading (and necessarily no Doppler shifts originating from the surface) and no discontinuities or ‘fading’ of individual transmission paths.

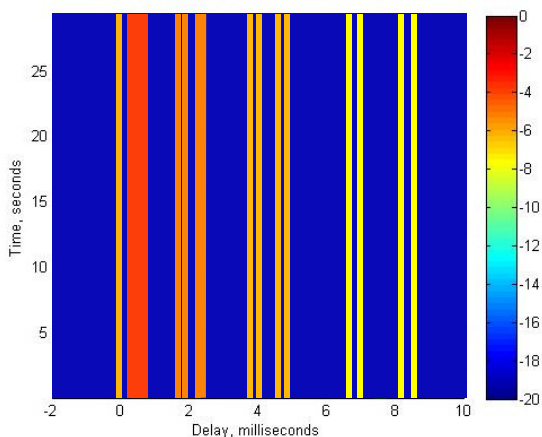


**Figure 3.** Illustrative static channel transmit-receive response history(dB) – 500 m range

## CHALLENGES EXTENDING STATIC CHANNEL METHODS TO A DYNAMIC CHANNEL

This section addresses some key problems with adapting a ray-propagation method developed for a static channel to a rapidly changing real channel.

### Summary of underlying static channel propagation method

The Bellhop (Porter and Bucker, 1987, Porter, 2011) ray-propagation model is being utilised as the basis of a dynamic simulation. This code is useful as it enables propagation calculation for range-dependent water-surface and bottom profiles. The range-dependent surface allows successive static surface-profile ‘instances’ to be modelled.

In ‘geometric’ mode this code models the propagation of a fan of ray-‘tubes’ that trace the path of points normal to propagating wave-fronts. Ray-tubes that bracket the receiver point represent a sound transmission path, and are utilised to calculate the total source level at the receiver. Examples of such rays are illustrated in Fig. 4. The amplitude at the receiver is calculated by considering the divergence of the ray-tube boundaries. The net phase change from boundary interactions is tracked for each ray-path as is the number of surface and bottom reflections, and the total flight-time for source to receiver, also referred to as the path delay.

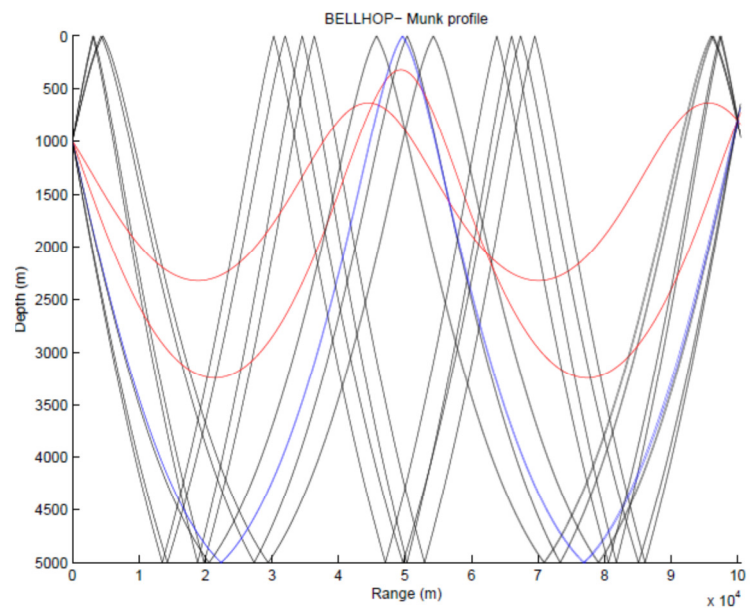


**Figure 4.** Example ray-trace using Bellhop model – image source (Porter, 2011)

### Validity of linear time-invariant (LTI) channel response convolution

The time-invariance of a static channel allows an arbitrary time-varying input signal  $p(t)$  (such as from an UW communications transmitter) to be convolved with a static channel response  $h(\tau)$  determined from geometrical analysis, to generate the time-varying channel output  $q(t)$  at a receiver as per (1), where  $\tau$  is the delay relative to the continuous transmit time  $t$ . The ‘linear’ characteristic indicates that the channel output signal magnitude varies proportionally to the input magnitude.

$$q(t) = \int_{-\infty}^{\infty} p(\tau)h(t - \tau) dt \quad (1)$$

By considering a signal that commences at  $t = 0$  and substituting  $t - \tau$  for  $\tau$ , then discretizing (1) such that the discrete complex amplitude response for the  $n$ th delay interval  $A_n = h(\tau)\Delta\tau$ , (1) becomes a summation of delayed and scaled replicas of the input signal  $p(t)$  as per (2).

$$q(t) = \sum_{n=1}^N A_n p(t - \tau_n) \quad (2)$$

To model the output  $q(t)$  from a time-varying channel it would be helpful if the real time-varying ocean channel could be approximated as a time-series of static channels, since there are well established techniques for determining the response  $h(\tau)$  of a static channel. The validity of this proposition has been examined by considering a nominal channel update period of 20 ms, and propagation ranges of 0.1 m, 1 km and 10 km.

The 20 ms time-step has been selected as a starting point for the channel impulse response update interval, based on the experimental channel coherence analysis presented by the authors in (Caley and Duncan, 2013). Others (Dol et al., 2012, Siderius and Porter, 2008) have previously described using rapid iterations of channel response for successive ‘frozen’ surface profiles to create a dynamic sea-surface simulator, utilising 10ms (Dol et al., 2012) and 12.5 ms (Siderius and Porter, 2008) time-steps between successive surface-realisation impulse responses.

Using a nominal acoustic sound-speed in water of 1500 m/s, a sound-wave will travel 30 m during a 20 ms time-step. Thus the actual acoustic flight-time for 0.1 km, 1 km and 10 km channel ranges would consist of approximately 3, 33 and 333 time-steps respectively. So even for the shortest 0.1 km channel, a wavelet would be less than half-way in its flight through the simulated channel before we want to update the channel response.

The conflict here is that the channel response at 20 ms intervals would be calculated using a ray-tracing propagation model relating to sound travelling the entire length of the channel, not just the 30 m that sound could actually travel in 20 ms. This conflict has been noted by others (Dol et al., 2012, Siderius and Porter, 2008). Expressed simply, the real channel response changes to some degree during the full flight-time of a sound wavelet.

### ‘Snapshot’ versus ‘fly-through’ ocean surface

Whilst it is clearly not possible for a wavelet to travel the full length of a real channel before the surface has changed, it would in principle be possible to calculate a time-warped ‘fly-through’ surface profile  $Z(x, \theta, \tau)$  which represents the shape of the dynamic surface experienced by a wavelet launched at angle  $\theta$  at time delay  $\tau$  as it travels the length of the channel. Successive channel responses calculated at 20 ms intervals using this warped surface profile  $Z$  would maintain the time-invariant assumption implicit in (1). The drawback however is that for each 20 ms interval the time-warped channel surface would need to be calculated for each and every ray launch angle in the ray-propagation ‘fan’ prior to calculating path delays.

The computational burden in actually utilising a ‘fly-through’ surface leads to a question of whether a simpler ‘snapshot’ ocean surface would suffice. This question can be examined by considering the maximum positional error of surface waves from their true ‘experienced’ position implied by the ‘snapshot’ simplification.

Consider Fig. 5, which schematically shows an acoustic wavelet travelling at sound speed  $c$ , with surface waves travelling with the horizontal speed spectrum  $V_x$  dependent on the wave period  $T$ . For illustrative purposes 1m wavelength surface waves and 150m wavelength swells have been considered in a shallow (13.5 m) channel over 0.1 km, 1 km, and 10 km ranges  $R$ . The maximum modelled horizontal error  $\xi$  in wave position by adopting the ‘snapshot’ channel profile would logically occur close to the receiver (corresponding to the maximum time-of-flight or range) as per (3) and summarised in Table 1.

$$\xi = RV_x/c \quad (3)$$

Given that we are unable to experimentally know or predict the position (or frequency) of either surface waves or swell more accurately than the maximum positional error associated with the ‘snapshot’ assumption, this assumption is considered valid.

**Table 1.** Maximum wave positional error  $\xi$  from ‘snapshot’ surface profile approximation measured in surface wavelengths ( $\lambda$ )

Transmission Range (m)	$\lambda = 1 \text{ m}, T = 0.8 \text{ s}, V_x = 1.25 \text{ m/s}$ wind waves	$\lambda = 150 \text{ m}, T = 14 \text{ s}$ swells $V_x = 10.7 \text{ m/s}$
100	$0.08\lambda = 0.08 \text{ m}$	$0.005\lambda = 0.75 \text{ m}$
1,000	$0.8\lambda = 0.8 \text{ m}$	$0.05\lambda = 7.5 \text{ m}$
10,000	$8\lambda = 8 \text{ m}$	$0.5\lambda = 75 \text{ m}$

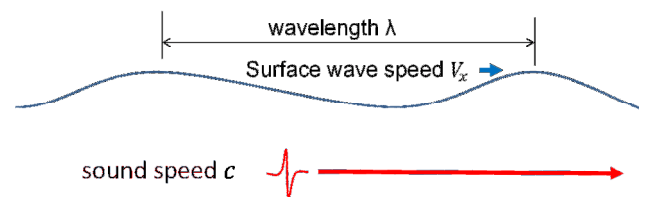


**Figure 5.** Sound speed interaction with surface horizontal wave speed

### Frequency dependence of ray-path modelling

Communication signals are typically designed to be wide-band both to maximise the data transfer rate, and to minimise vulnerability to frequency-selective channel fading. The signal band width may be as wide as 50% of the centre frequency. Thus a signal centred on carrier  $f_0 = 12 \text{ kHz}$  may typically contain frequency components extending from 9 kHz to 15 kHz. If the bottom reflection coefficient was strongly dependent on frequency at communication frequencies it would be difficult to validly use the multi-path arrival delay and amplitude data from a single-frequency run of a ray-propagation model to synthesise the channel response for a broad-band communication signal. Fortunately the bottom reflection coefficient is weakly dependent on frequency at communications frequencies as has been previously established (Siderius and Porter, 2006) by considering the difference in synthesised signal based on reflection coefficients calculated in a lower potentially more frequency sensitive range at 500 Hz and 5000 Hz. The authors in (Siderius and Porter, 2006) note that quite apart from the demonstrated frequency-insensitivity of the bottom reflection coefficient at relatively high frequency, the knowledge of the substrata that would be necessary to correctly predict the frequency-

dependency of the bottom reflection coefficient is generally not available.

### Path emergence and disappearance

The emergence and disappearance of transmission paths is the primary process that creates the intermittent real channel response illustrated in Fig. 2. The extent to which this phenomenon may be simulated deterministically is a key question to be answered in developing a simulator.

The complementary problem of identifying path delay variations from one impulse response to the next is critical to deterministically modelling transient Doppler. The Doppler induced frequency shift  $\delta f$  relative to the signal frequency  $f$  on a ray-path during interval  $\Delta t$  between successive calculated impulse responses, is determined by the change in path delay  $\Delta \tau$  as per (4).

$$\delta f/f = \Delta \tau/\Delta t \tag{4}$$

Ray-propagation models such as Bellhop (Porter and Bucker, 1987, Porter, 2011) provide useful geometrical, amplitude, delay and phase information for transmitting ray-paths that can help identify transient changes in these properties on continuing paths, however due to the unlimited complexity of real surface profiles it is not possible to exactly match continuing paths based on logical criteria. For example, a continuing path will likely have the following characteristics from one impulse response to the next:-

- a) same number of surface and bottom reflections, and
- b) plausible change in launch ray angle, and
- c) plausible change in received ray angle
- d) plausible change in delay

A criterion could also be added limiting the net change in path phase from all boundary interactions, however this is implicitly achieved by the condition a) above requiring the same number of surface and bottom reflections.

Referring to Fig. 6, the test of a plausible launch angle during interval  $\Delta t$  is based on the assumption that a continuing ray-path may experience a moving reflection point consistent with the maximum horizontal speed  $V_{xmax}$  of surface waves (i.e. swell). This may be estimated from the water depth in shallow water, or from the surface-wave spectrum in deep water. The resulting condition for a transmitter at depth  $D_{tx}$  is given by (5). A similar condition can be developed at the receiver. Criteria for angular changes can be elaborated to include the effects of transmitter and receiver motions.

$$D_{tx} \left| \left( \frac{1}{\tan \theta_i} \right) - \left( \frac{1}{\tan \theta_{i+1}} \right) \right| < V_{xmax} \Delta t \tag{5}$$

As the channel range/depth aspect ratio increases and the launch angle of transmitting paths becomes shallow it becomes increasingly difficult (i.e. impossible) to unambiguously match continuing paths from one channel ‘snapshot’ to the next. Any angular criterion that may be developed to try and exactly match paths becomes more sensitive than the ray-propagation path angular spacing and therefore unusable. Initial thoughts were that the methodology should be abandoned for lack of determinism, however to do so also abandons attempts to deterministically model Doppler via delay changes. The alternative view that has been pursued is that if path similarity reaches the point that the matching of paths is ambiguous, it is likely that there will be little observable difference in model output no matter which paths are matched.

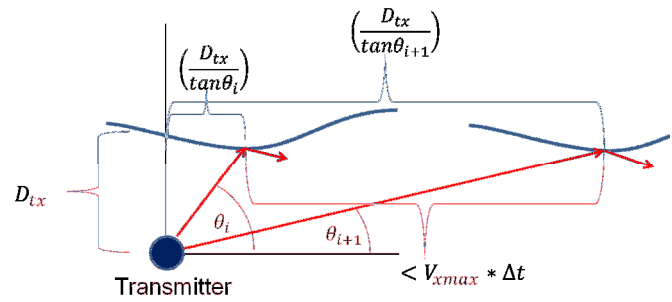


**Figure 6.** Launch angle criterion (5) for identification of a possible continuing ray-path reflection off a travelling wave between successive impulse responses spaced by  $\Delta t$

### Seamless signal simulation from discrete-interval impulse responses

To produce a wide-band signal simulation that is free from spectral aberrations it is desirable that the simulation does not artificially introduce response discontinuities at frequencies less than the signal sample rate. For a simulation based on 96 kilosamples/second signal input and 20 ms impulse response update interval, there are 1920 signal samples between successive impulse response updates. The channel response parameters for each continuing path (amplitude, phase and delay) must therefore be interpolated between impulse responses at the sample rate. The same is also true for emergent and vanishing paths.

For continuing paths all three parameters can be interpolated. However for an emergent path or a diminishing path there is only information available to interpolate the amplitude either increasing from zero, or diminishing to zero.

### PATH-BASED SIMULATION STRUCTURE

A time-domain simulation based on (2) has been developed to convolve an arbitrary continuous input signal (nominally within a 8 kHz to 16 kHz bandwidth) with the time varying amplitude, phase and delay response of discrete ray propagation paths. This structure is shown schematically in Fig. 7.

Conceptualising individual paths enables focus on the identification of continuing and discontinuing paths between successive channel impulse responses, which forms the basis of simulating transmission intermittency and signal Doppler shifts through path range variation.

The input signal is converted to quadrature form by a Hilbert transform before being stored in an input signal buffer that provides an ‘analogue’ of the time of flight between a transmitter and receiver. The buffer allows transient increases and decreases in path range to be expressed through transient changes to the delay  $\tau$  on a given path. The input buffer in quadrature enables continuous incorporation of Doppler for a given path by fractional interpolation of the signal between successive samples.

Simulation of discrete transmission paths provides the opportunity to dynamically update parameters representing transient physical processes that are differentiated across the range of propagation paths. In particular, surface-interacting paths will experience changes in response depending on sea-state and path launch angle that will not be experienced by other paths.

A time-varying Finite Impulse Response (FIR) filter has been incorporated into each ray path to provide a mechanism to

add transient characteristics that are not captured by successive impulse responses determined from ray-tracing, which has limited capacity to address complex surfaces with short-wavelength wind-waves.

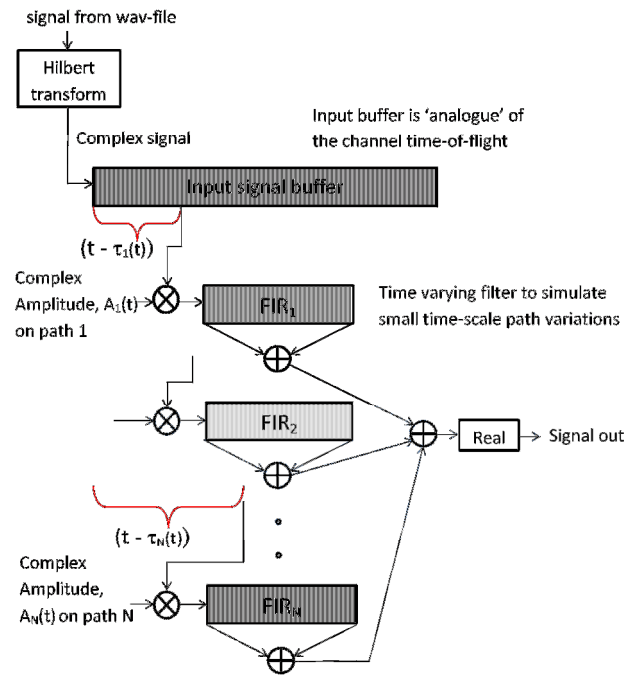


Figure 7. Conceptual time-domain channel simulation

**Similar transient models**

Siderius and Porter (Siderius and Porter, 2008) have described a methodology for interpolating the Bellhop static channel arrival data on a two-dimensional grid (range and depth) to simulate arbitrary transmitter or receiver movements with a dynamic sea surface. Ray-path arrival data is pre-calculated on a 2D arrival data grid each 12.5 ms to simulate the response to a transient sea-surface profile. The response at intermediate points in space and time are interpolated from arrival data computed at 8 grid vertices. The authors note that the model is suited to conditions of swell and moderate seas. (For comparison, the methodology presented in this paper interpolates arrival data between two successive arrival points that are coincident with the tx-rx trajectory). For rough seas the ray-tracing methodology presented by (Siderius and Porter, 2008) is replaced with a Kirkoff approximation method for computing the 2D sound field each time-step. The methodology is limited to cases with either a fixed transmitter or receiver.

Dol et al (Dol et al., 2012) also describe a similar methodology for using successive Bellhop arrivals calculated for static ‘snapshot’ channels, updated each 10ms. Their modelling has focussed particularly on simulating the effects of dynamic sea surfaces on communication signals, including the effects of bubble-entrainment from breaking waves on the sound-speed profile, with fixed transmitter and receiver positions.

**PRELIMINARY MODELLING RESULTS**

Simulation modelling has commenced with a flat sea-surface scenario and arbitrary transmitter and receiver movements. This scenario readily demonstrates the path-matching methodology, as the simple ray-path geometry results in unambiguous correspondence of ray paths (i.e. path-matching) from one impulse response to the next.

The example presented in Fig. 8 simulates the signal distortion over a 20 second interval during which a transmitter travelling at 10 m/s passes by a receiver at a closest approach range of 100 m in 13.5 m iso-velocity water depth. The channel response update interval was 20 ms.

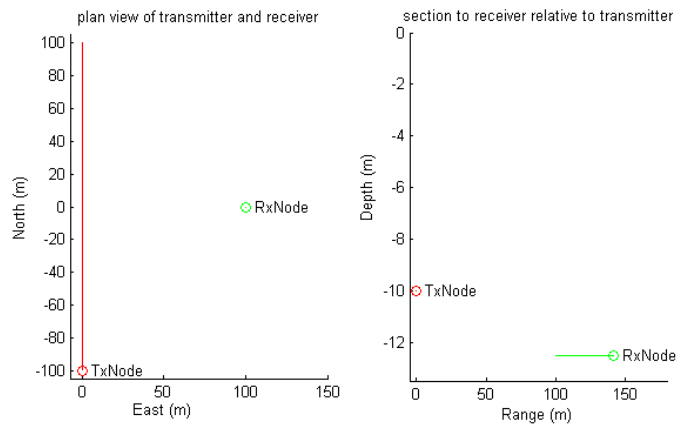


Figure 8. Relative transmitter-receiver pass-by trajectory in plan and cross-section views

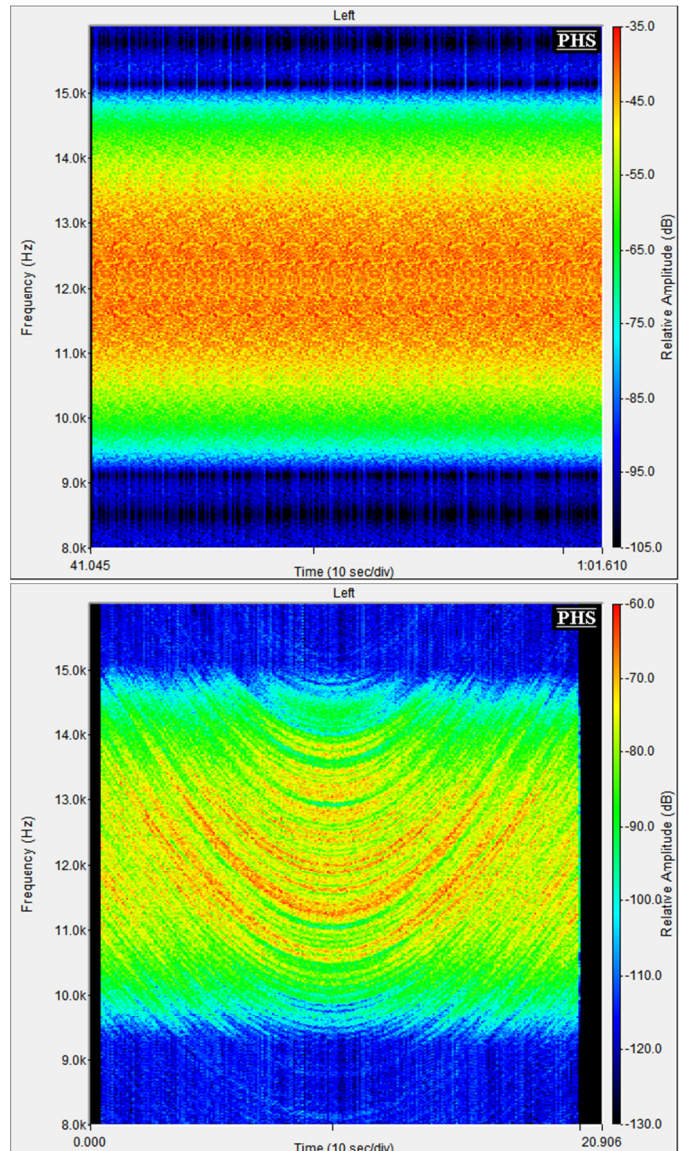
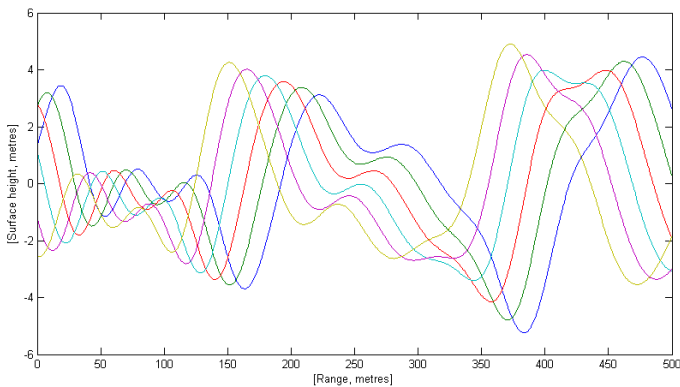


Figure 9. Transmit signal spectrogram at 1m (top), and receive signal spectrogram (bottom)

A 20 second sample of a transmitted broad-band communication signal and simulated received signal spectrogram is presented in Fig. 9. This example successfully replicates the variable frequency-selective fading and ‘bathtub’ spectrogram appearance that is characteristic of the received underwater signal during pass-by of an underwater noise. Simulation over the same range with a multi-tone signal (8 kHz, 10 kHz, 12 kHz, 14 kHz, 16 kHz) demonstrated the correct frequency dependent Doppler shift generated by the transient propagation range.

The path-matching methodology has also been tested with less success for fixed transmitter and receiver at the same depths, but with a moving sea-surface. Fig. 10 illustrates the first 5 seconds of simulated 2-dimensional surface-wave evolution for a very large swell (~9 m) over a 500 m range. The resulting 20 second duration received signal spectrograms for the same source signal over 100 m and 500 m ranges are illustrated on Fig. 11.



**Figure 10.** Example 5-second ‘snapshots’ of surface evolution with a 9m swell

At short range (100 m, top of Fig. 11) the frequency-selective fading is evident as path-lengths expand and contract. At longer range (500m, bottom of Fig. 11), whilst it is not clearly evident from the presented spectrogram, the numerical simulation results indicate an absence of path-matching from one channel response to the next, resulting in a loss of simulation of any transient Doppler shift. The simulation has however produced transient signal strength variations associated with swell focusing effects, which is realised as a transient increase in the number of transmission paths.

**FUTURE MODELLING WORK**

Preliminary modelling work has highlighted the limitations of deterministic modelling based on explicit ray-path identification for complex surfaces. In particular, the path-matching approach to transient Doppler will be supplemented with the path delay interpolation method described by Siderius and Porter (Siderius and Porter, 2008) that does not depend on explicit path-matching.

Key challenges for future work include:- i) channel simulation for realistic time-series sets of surface wave realisations, to enable the synthetic channel response to be compared with experimental channel response data from probing trials that have been conducted to date. (Experimental transient channel responses have been measured for a 13.5 m deep channel at ranges of 50 m to 1000 m, and for a 50 m deep channel at ranges of 250 m to 10,000 m.); ii) comparison of the synthetic channel statistics with the measured channel to establish

the channel behaviour that is not being captured by deterministic methods; and iii) to develop an approach to incorporating fine time-scale path responses associated with short wavelength wind-driven surface waves.

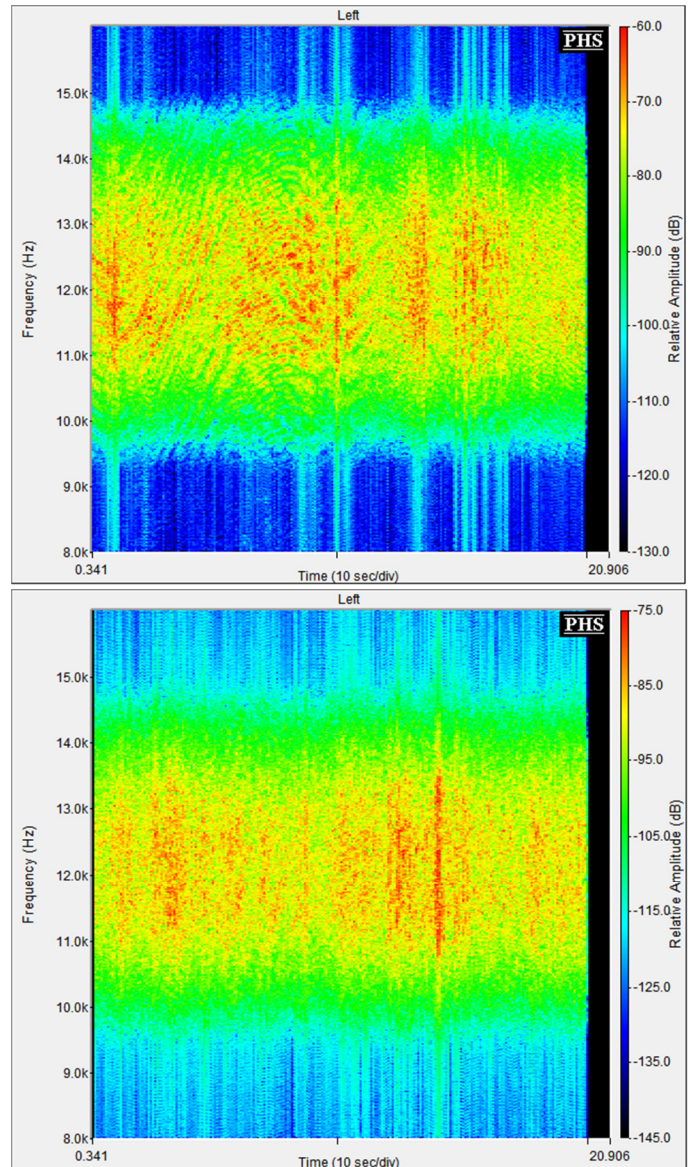


**Figure 11.** Spectrogram of simulated received signal at 100 m range (top), and 500 m range (bottom) resulting from moving sea surface (Fig. 10)

**SUMMARY**

This paper presents a methodology for extending an existing ray-path sound propagation modelling technique (Bellhop) developed initially for static channel geometries, to model the fine timescale transient effects of a dynamic ocean channel. The key phenomena that are missing from a channel simulation based on a static channel are the differential transients in arrival time on different transmission paths (delay spreading) which are synonymous with transient Doppler shifts in arriving signal ‘packets’ (Doppler or frequency spreading), and the intermittency of transmission paths.

The modelling approach that has been described aims to reproduce Doppler and delay spreading and intermittency of

the arriving signal stream in a path-based deterministic manner. This deterministic model component will be implemented as far as practicable, consistent with available computing power. Those stochastic elements of the model that cannot be practicably incorporated through ray-based modelling with surface profile realisations will be addressed next after evaluating the fidelity of the deterministic part of the model.

The structuring of the deterministic and stochastic elements of the model based on individual transmission paths is being pursued to provide maximum opportunity to incorporate available knowledge of path-dependent physical acoustic interactions.

## ACKNOWLEDGMENTS

This project is supported under the Australian Research Council's Discovery Projects funding scheme (project number DP110100736) and by L3-Communications Oceania Ltd.

## REFERENCES

- Caley, MS & Duncan, AJ 2013, 'Investigation of underwater acoustic multi-path Doppler and delay spreading in a shallow marine environment', *Acoustics Australia*, vol. 41, no. 1, pp. 20-28.
- Dol, HS Colin, MEGD Ainslie, MA Van Walree, PA & Janmaat, J 2012, 'Simulation of an underwater acoustic communication channel characterized by wind-generated surface waves and bubbles', Proceedings of the Underwater Communications Channel Modelling and Validation (UComms) conference, NATO Centre for Maritime Research and Experimentation, 2012 Sestri Levante, Italy.
- Eggen, TH Baggeroer, AB & Preisig, JC 2000, 'Communication over Doppler spread channels - Part I: Channel and receiver presentation', *IEEE journal of oceanic engineering*, vol. 25, pp.62-71.
- Nordholm, S Rong, Y Huang, D & Duncan, AJ 2010, Increasing the range and rate of underwater acoustic communication systems using multi-hop relay. Curtin University: Australian Research Council Discovery Project DP110100736
- Porter, MB 2011, The BELLHOP Manual and Users Guide - preliminary draft. HLS Research, La Jolla, CA, USA.
- Porter, MB & Buckner, H P 1987, 'Gaussian beam tracing for computing ocean acoustic fields', *Journal of the Acoustical Society of America*, vol. 82, no. 10.
- Siderius, M & Porter, MB 2006, 'Modeling techniques for marine-mammal risk assessment', *IEEE journal of oceanic engineering*, vol. 31, pp. 49-60.
- Siderius, M & Porter, MB 2008, 'Modeling broadband ocean acoustic transmissions with time-varying sea surfaces', *Journal of the Acoustical Society of America*, vol. 124, no. 1, pp.137-150.
- Van Walree, PA Jenserud, T & Smedsrud, M 2008, 'A Discrete-Time Channel Simulator Driven by Measured Scattering Functions', *IEEE journal on selected areas in communications*, vol. 26, pp. 1628-1637.